PPPL--2630

DE89 014601

Pulse Length Assessment of Compact Ignition Tokamak Designs

D. P. Stotler and N. Pomphrey
Princeton Plasma Physics Laboratory
Princeton University
Princeton, New Jersey 08543

ABSTRACT

A time-dependent zero-dimensional code has been developed to assess the pulse length and auxiliary heating requirements of Compact Ignition Tokamak (CIT) designs. By taking a global approach to the calculation, parametric studies can be easily performed. The accuracy of the procedure is tested by comparing with the Tokamak Simulation Code [S. C. Jardin, N. Pomphrey, and J. De Lucia, *J. Comput. Phys.*, 66, 481 (1986)] which uses theory-based thermal diffusivities. A series of runs is carried out at various levels of energy confinement for each of three possible CIT configurations. It is found that for cases of interest, ignition or an energy multiplication factor $Q \gtrsim 7$ can be attained within the first half of the planned five-second flattop with 10 - 40 MW of auxiliary heating. These results are supported by analytic calculations.

I. Introduction

Present designs of the Compact Ignition Tokamak[1] (CIT) are limited to a current flattop time of five seconds due to resistive heating of the toroidal field coils and other factors. Some of these five seconds will be needed to complete the plasma heating process begun during the current ramp phase. The rest of the flattop time will then be available for studying the physics of an ignited plasma. In this paper, we provide an estimate of the length of this period for three possible CIT configurations.

The time required to heat the plasma to ignition temperatures is directly related to the amount of auxiliary power available. So, we can equivalently view this study as yielding the level of auxiliary heating needed to obtain a certain value of the heating time.

Previous work along these lines employed complicated (and time-consuming) 1-1/2-D transport simulations.[2,3] Since reliable transport models for this task do not exist in fully validated form, it is not clear that the extra effort required to proceed with these simulations would be worthwhile. Instead, we will employ a code designed to follow the time evolution of the volume-integrated plasma energy. This approach results in a significant decrease in the time needed to analyze a particular discharge scenario. Hence, a number of studies spanning the envisioned parameter space can be carried out easily.

As has been pointed out elsewhere (see Ref. 4 and references therein, for example), the level of energy confinement in CIT is the most uncertain element in this type of calculation. If the thermal insulation is below a certain amount, it will be difficult to attain values of the energy multiplication factor Q much in excess of unity without extraordinary auxiliary heating power (say, > 40 MW). On the other hand, if the energy confinement is above some larger value, CIT should ignite readily with little or no auxiliary power input. The questions we wish to answer are relevant only in a band of energy confinement between these two extremes.

In this range, we find for each of the CIT designs that $Q \gtrsim 1$ or ignited operation can be achieved within the first half of the flattop for 10 - 40 MW of auxiliary power. Detailed results are presented in a table.

Several aspects of this problem are amenable to analytic solution. We will present two simple models that show qualitatively how the time needed to

heat the plasma depends upon the auxiliary power available, the minimum auxiliary power required, plasma density, etc. A formula for the minimum power required to achieve ignition has been developed by Waltz et al.[5]; we will apply it to our assumed energy confinement scaling. Finally, we will consider the consequences of using an energy confinement formula that depends upon the input power rather than the plasma energy, as is assumed for the bulk of this work.

In Sec. II, we describe our global, time-dependent code and present a comparison with a sophisticated transport code. Section III contains the results of a parametric study for three different CIT designs. The analytic calculations are presented in Sec. IV. Finally, we provide a summary in Sec. V.

II. Time-Dependent Global Code

A number of global power balance codes have been developed recently.[5-9] They typically solve an equation similar to

$$P_\alpha + P_{OH} + P_{aux} = P_{con} + P_{rad}. \tag{1}$$

The individual terms represent the volume-integrated contributions made to the total power balance by alpha, ohmic, and auxiliary heating; thermal conduction and radiated losses are on the right-hand side.. We generalize this expression to include time dependence and helium ash accumulation:

$$\frac{dW_{tot}}{dt} = -P_{con} - P_{rad} + P_\alpha + P_{OH} + P_{aux}, \tag{2}$$

$$\frac{dN_{He}}{dt} = \frac{P_\alpha}{E_\alpha} - \frac{N_{He}}{\tau_{p,He}}. \tag{3}$$

The various terms in Eq. (2) will be described below. In Eq. (3), N_{He} is the number of helium ash particles, $E_\alpha = 3.5$ MeV is the alpha birth energy, and $\tau_{p,He}$ is the (constant) helium ash particle confinement time. Equation (3) assumes that the slowing down of fast alpha particles takes place instantaneously. In reality, the alpha slowing-down time in CIT is expected to be on the order of 100 msec.

Codes such as the one described here are zero-dimensional (0-D) in that the plasma profiles are all specified on input. We will use for density, temperature, and plasma current density

$$x = x_0(1 - r^2/a^2)^{\alpha_x}, \tag{4}$$

where x is replaced by n, T, and J, respectively; a is the plasma minor radius. Then, the alpha power is computed using

$$P_\alpha = E_\alpha 4\pi^2 R\kappa \int_0^a r\,dr\, n_D n_T \overline{\sigma v}_{DT}, \tag{5}$$

where R is the plasma major radius, and κ is the plasma elongation. The reactivity, $\overline{\sigma v}_{DT}$, is calculated with a formula obtained by Hively[10] in order to ensure correct results in all temperature regimes. Consequently, this integral must be computed numerically for each value of the density-weighted, volume-averaged temperature, $\langle T\rangle \equiv \langle n_e T\rangle/\langle n_e\rangle$.

The ohmic heating power is (all powers are in watts)

$$P_{OH} = \frac{4.17\times 10^3 Z_{eff}\ln\Lambda\gamma_{NC}T_0^{-3/2}V}{1+2\alpha_J-\frac{3}{2}\alpha_T} \times\left\{\frac{B_T[1+\kappa^2(1+2\delta^2-1.2\delta^3)]}{2\kappa R q_0}\right\}^2, \tag{6}$$

where Z_{eff} is the effective charge, $\ln\Lambda$ is the Coulomb logarithm, γ_{NC} is the neoclassical resistivity enhancement factor (constant, taken to be 2.5), T_0 is the central electron (and ion) temperature in keV, B_T is the toroidal magnetic field in tesla, R and a are in metres, δ is the triangularity, and V is the plasma volume in m^3. This expression for P_{OH} is essentially the same as that used by Uckan.[9]

We will assume that the safety factor on axis, $q_0 = 1$ and compute $\alpha_J = q_{cyl}/q_0 - 1$. For the equivalent cylindrical safety factor, we take

$$q_{cyl} = \frac{5a^2 B_T}{RI_p}\frac{[1+\kappa^2(1+2\delta^2-1.2\delta^3)]}{2}, \tag{7}$$

where I_p is the plasma current in mega-amperes. These units will be used throughout this paper unless otherwise specified.

Only bremsstrahlung radiation is included[9] in P_{rad}:

$$P_{rad} = 5.31 \times 10^{-37} \frac{n_{e0}^2 T_0^{1/2} Z_{eff} V}{(1 + 2\alpha_n + \frac{1}{2}\alpha_T)}, \tag{8}$$

where n_{e0} is the central electron density.

Finally, the conducted losses are written as

$$P_{con} = \frac{W_{tot}}{\tau_E} = \frac{2.40 \times 10^{-16} \left(\langle n_e T \rangle + \langle n_i T \rangle\right) V}{\tau_E}. \tag{9}$$

The time dependence of P_{aux} (the auxiliary heating power), Z_{eff}, I_p, B_T, $\langle n_e \rangle$, and the plasma boundary shape are specified on input. We assume that there is one impurity of charge Z in addition to the helium ash. From the electron density, Z_{eff}, Z, and the helium ash density, we can compute the amount of hydrogen in the plasma, taken to be 50% deuterium and 50% tritium. Constant values of α_n and α_T are prescribed as well. Then, given initial conditions for W_{tot} and N_{He}, Eqs. (2) and (3) can be integrated using standard techniques.

In order to estimate the accuracy of this procedure, we compare a simulation of CIT produced by the Tokamak Simulation Code[11] (TSC) with results from our code. TSC is being used to evaluate the magnetics design for CIT. In addition to the free boundary equilibrium calculations required for this task, it carries out a complete time-dependent, 1-1/2-D transport calculation.

We need to make two minor modifications to our 0-D code to match features present in TSC. First, a global calculation of the cyclotron radiation is included in P_{rad}. Second, a feedback loop is installed to adjust P_{aux} to maintain a total input power $P_\alpha + P_{aux} + P_{OH} \leq 110$ MW. Neither of these are used in the calculations described in Sec. III.

The specific TSC simulation with which we will be comparing is designated as F11D1. It is similar to the one described in detail in Ref. 12. From the TSC output, we take the field and shape ramps, shown in Fig. 1. The auxiliary power programming is included in Fig. 2; 15 MW of auxiliary power is input at $t = 4.5$ s, and another 15 MW is added at $t = 7.5$ s. The falloff of P_{aux} for $t > 7.5$ s is the result of the feedback loop explained above. The volume-averaged electron density is brought up linearly in time from $\langle n_e \rangle = 0$

at $t = 0$ to $\langle n_e \rangle = 3.1 \times 10^{20}$ m^{-3} at $t = 7.5$ s and held constant thereafter. The density and temperature profiles TSC obtains do not vary greatly during the simulation. We choose our profile peaking factors using

$$\frac{n_0}{\langle n \rangle} = 1 + \alpha_n,$$

and

$$\frac{T_0}{\langle T \rangle} = \frac{(1 + \alpha_n + \alpha_T)}{(1 + \alpha_n)},$$

arriving at $\alpha_n = 0.58$ and $\alpha_T = 1.53$. As in TSC, we employ $Z_{eff} = 1.5$, $Z = 8$, and $\tau_{p,He} = 1$ s.

It remains only to specify the form of τ_E. TSC uses a generalization of the Tang transport model based on drift-wave turbulence.[13,14] The TSC expression for the thermal diffusivity $\chi(r)$ consists of two pieces, one for the ohmic regime and one for the auxiliary heated regime. The two are combined in a sum of squares sense. To get a corresponding global model, we write

$$\tau_E^{-2} = \tau_{NA}^{-2} + (c_\tau \tau_{aux})^{-2}, \tag{10}$$

where τ_{aux} is the scaling for auxiliary heated plasmas, and

$$\tau_{NA} = 7 \times 10^{-22} \overline{n}_e a R^2 q_{cyl} \tag{11}$$

is the neo-Alcator (ohmic) contribution, with $\overline{n}_e$ being the line-averaged electron density. The constant multiplier c_τ is specified on input.

We will use the Kaye-Allen-Complex L-mode scaling[4,15] for τ_{aux},

$$\tau_{aux} = \tau_E^{KAC} = 0.0521\, \overline{A}_i^{0.5} \kappa^{0.25} I_p^{0.85} \overline{n}_{e,19}^{0.1} B_T^{0.3} a^{0.3} R^{0.85} P_{in}^{-0.5}, \tag{12}$$

where $\overline{A}_i$ is the average ion mass (taken to be 2.5). $\overline{n}_{e,19}$ is the line-averaged electron density in units of 10^{19} m^{-3}, and $P_{in} = P_\alpha + P_{OH} + P_{aux} - P_{rad}$ is the net input power in megawatts. We intend for this P_{rad} to refer only to centrally peaked radiation mechanisms, such as bremsstrahlung, that affect the power balance in the center of the plasma. We evaluate τ_{NA} and τ_E^{KAC} at one point during the flattop of the TSC simulation and choose c_τ so that Eq. (10) yields the simulated value of τ_E. This procedure leads to $c_\tau = 1.9$.

The results of the comparison between the 0-D model and TSC are shown in Fig. 2. We first note that the 0-D estimate of P_{OH} is $\sim$ 1 - 2 MW too

large. Possible causes for this discrepancy are differences in current profile shape, flux surface shape, and neoclassical resistivity treatment. The total radiated power P_{rad} matches very well throughout. The alpha power P_α is $\sim 10\%$ larger in the 0-D code than in TSC. This is due to differences in the density and temperature profile shapes, as well as differences in the plasma volume. The conducted powers agree by virtue of the feedback loop on P_{aux} and the choice of c_τ.

The error in the power balance brought on by the difference in P_α is absorbed by P_{aux} via the feedback loop. In particular, note that $P_{aux} < 0$ in the 0-D code. From the point of view of Eq. (2), there is nothing peculiar about this. While physically unrealistic, it does allow us a clear comparison of the two simulations. In particular, we conclude that our error is about 10 MW out of 110 MW total input power, $\sim 10\%$.

III. Parametric Study for CIT

We examine three proposed magnetic configurations for CIT:

1. $I_p = 9$ MA, $B_T = 8.2$ T — present CIT design with existing TFTR power supplies.
2. $I_p = 11$ MA, $B_T = 10$ T — present CIT design with upgraded power supplies.
3. $I_p = 13$ MA, $B_T = 11.8$ T — possible enhanced design using a bucked coil design.

For all three designs, $R = 2.1$ m, $a = 0.65$ m, $\kappa = 2$, and $\delta = 0.4$. The magnetic fields have been chosen in cases (1) and (3) to yield the same value of q_{cyl} as in case (2), $q_{cyl} = 2.73$. We take the field and shape ramps for the 11 MA device from the TSC run F11D1 (Fig. 1) and rescale the I_p and B_T programming for the other two cases.

The input parameters are as in Sec. II with the following exceptions. The energy confinement time is written as

$$\tau_E = \min\left[\tau_{NA}, c_\tau^2 \tau_E^{KAC}(W_{tot})\right]. \tag{13}$$

This expression is more appropriate since the database from which τ_E^{KAC} is derived contains numerous low power discharges.[16] The neo-Alcator contribution is included only to provide a reasonable behavior when $\langle n_e \rangle$ and $\langle T \rangle \rightarrow 0$. We have also rewritten the scaling in terms of the plasma energy instead of the input power. The means of doing this and its consequences will be described in Sec. IV.C. The multiplier c_τ is squared in Eq. (13) as a result of the conversion procedure. It is still a *linear* multiplier on the power form of τ_E^{KAC}. In the results described below, c_τ will be varied systematically.

Another difference with Sec. II is that instead of assuming a step function increase, we ramp the auxiliary heating power linearly with time between $t = 4.5$ s and 5.5 s. This is a more plausible representation of the increase in heating efficiency expected to take place as the ICRF resonance layer moves toward the plasma center during the magnetic field ramp. The auxiliary power is held constant thereafter. We can vary the amount of heating and the length of time it is on. For ignited cases, we remove the auxiliary heating once the discharge has reached the point of ignition. For slightly sub-ignited cases, we suddenly reduce P_{aux} at some point during the current flattop in order to operate at $Q \gg 1$. In all other instances, the auxiliary heating remains at full power until the end of the run.

As will be demonstrated in more detail in Sec. IV.B, the performance of CIT is very sensitive to the value of c_τ. Given that it would be unrealistic to plan for much more than 40 MW of auxiliary power on CIT, we are restricted in how small c_τ can be in order to attain $Q > 5$ operation. Below this level of confinement, the most desirable operating point (with $P_{aux} \leq 40$ MW) is at a sufficiently low temperature that the time needed to heat the plasma is short. Likewise, above some larger value of c_τ, ohmic ignition is possible. In this case, the time required to reach ignition, perhaps with a small amount of auxiliary power, is short enough that it is, again, pointless to do the calculation. We examine three values of c_τ lying between these two extremes.

For each c_τ, we consider separately two values of P_{aux}, $10 \leq P_{aux} \leq 40$ MW, in order to give some idea of the range of modes of operation possible at that level of confinement. We pick the flattop $\langle n_e \rangle$ to yield the highest Q or quickest ignition at each auxiliary power level. We require that the

line-averaged density be less than[17]

$$\overline{n}_{e,max} = \frac{2B_T}{Rq_e}\, 10^{20}\mathrm{m}^{-3}, \tag{14}$$

where $q_e = 5a^2\kappa B_T/RI_p$ is the engineering q value. As in the TSC comparison, the density is ramped linearly from zero between $t = 0$ and $t = 7.5$ s.

For each of the three CIT configurations, there are three c_τ values, each run with two levels of auxiliary heating. This makes a total of 18 simulations. The results are summarized in Table I. The first three columns provide the L-mode multiplier c_τ, P_{aux} in MW, and the flattop density in units of 10^{20} m^{-3}, $\langle n_{e,20}\rangle$. The maximum values of P_α and Q occurring during the simulations are given. Ignited cases are indicated by $Q_{max} = \infty$; the time at which the auxiliary heating is turned off is also given for these runs. The time of maximum P_α (ignited cases) is presented in the last column. As will be demonstrated in Sec. IV.A, a finite Q state is approached logarithmically in time (ignoring He ash buildup), and much of the flattop is spent attaining the last few increments in Q. So, we take the $90\%\, Q_{max}$ point as characterizing the time required to heat the plasma in these cases. The $Q \gg 1$ simulations are distinguished by the additional entry "@ x MW" in the Q_{max} column. For these runs, P_{aux} is reduced to x MW at some point prior to $t(0.9Q_{max})$ and held there for the remainder of the discharge.

As examples, we present in Figs. 3 - 5 results for the 11 MA configuration with $c_\tau = 1.6$. In Fig. 3, the contours of constant auxiliary power (in MW) required to maintain steady state at a given $\langle n_e\rangle$ and $\langle T\rangle$ are plotted (see, for example, Refs. 6 and 9). This type of diagram is referred to as a Plasma OPeration CONtour or POPCON plot.[18] The density and β limits ($\beta_{max}(\%) = 3I_p/aB_T$) are also indicated. Figure 3 is constructed using the flattop parameters (i.e., $t \geq 7.5$ s) and does not assume any helium ash buildup. For this c_τ, we examine $P_{aux} = 20$ and 30 MW. The densities for these cases are $\langle n_{e,20}\rangle = 3.8$ and 4.3, respectively.

The time dependence of the terms in Eq. (2) for the 20 MW case is shown in Fig. 4. According to Fig. 3, this case should be ignited. But, there is sufficient helium ash buildup ($n_\alpha/n_e = 0.014$ at $t = 12$ s) during the discharge to close the relatively small ignition window present at this density. However, $Q \gg 1$ operation is possible. So, when $\langle T\rangle$ reaches ~ 9

keV ($t = 8.6$ s), we reduce P_{aux} to 2 MW. At the end of the run, $\langle T \rangle = 9.7$ keV.

By raising the density to the maximum allowed, $\langle n_e \rangle = 4.3 \times 10^{20}$ m^{-3}, we can achieve ignition at this value of c_τ (Fig. 5). To overcome the increased thermal inertia without having to heat through most of the flattop, however, we need to raise P_{aux} to 30 MW. We turn off the auxiliary heating when $\langle T \rangle \simeq 9$ keV. Again, the helium ash buildup ends the ignition soon after it starts. By the end of the calculation, $\langle T \rangle$ drops to 8.5 keV.

With the freedom to vary P_{aux} between 10 and 40 MW and to choose any operating density below the prescribed density limit, we have been able to reach ignition (for the larger c_τ cases) or at least $Q \gtrsim 7$ within the first half of the flattop ($t < 10$ s) in most of the cases reported in Table I. Greater restrictions on the auxiliary power available, the density, the magnitude of c_τ, or on the fusion power could lead to scenarios in which the full flattop time is needed to reach the desired operating point.

IV. Analytic Calculations

Several aspects of this problem can be addressed analytically. We will develop two simple models to describe the time required to heat the plasma in terms of quantities found on a POPCON plot. By applying the results of Waltz, Dominguez, and Perkins[5] to the particular cases of interest here, we can understand why we find CIT performance to be so sensitive to c_τ. This same result can be used to show that if ignition can be achieved at all in CIT for these confinement and density scalings, the power required to reach ignition is $\lesssim 10$ MW. Finally, we will demonstrate that the use of a power-dependent confinement scaling instead of one written in terms of the plasma energy can almost double the required heating time.

IV.A. Time Required to Heat the Plasma

It is difficult to integrate Eq. (2) analytically in general. Some of the problem terms can be neglected, but the results still tend to be too complicated to provide insight. What we seek to do here instead is to model the most important structure displayed in POPCON plots (e.g., Fig. 3) in

such a way that Eq. (2) can be integrated exactly, yielding $W_{tot}(t)$ or at least $t(W_{tot})$.

We first consider cases in which ignition is possible within the prescribed density and β limits, Fig. 3 for example. The precise question we seek to answer is: how long does it take to heat from the ohmic equilibrium contour to the ignited equilibrium contour? This is, of course, dependent upon the path in $\langle n_e \rangle$ and $\langle T \rangle$ space.

We will assume for the moment that all parameters except for $\langle n_e \rangle$ and $\langle T \rangle$ are fixed during this process. Then, all of the variations in dW_{tot}/dt can be deduced from a POPCON diagram, i.e., a contour plot of

$$P_{pb}(\langle n_e \rangle, \langle T \rangle) \equiv \frac{W_{tot}}{\tau_E} + P_{rad} - P_{\alpha} - P_{OH}. \tag{15}$$

The subscript "pb" refers to power balance. In an ignited case, P_{pb} goes through a maximum along a constant density path between the ohmic and ignited equilibrium contours. We can model this behavior at least near the maximum with a parabola,

$$P_{pb} = a\langle T \rangle^2 + b\langle T \rangle + c. \tag{16}$$

By specifying P_{pb} at two points (for example, one on each of the ohmic and ignited equilibrium contours) and the maximum value, P_m, of P_{pb} along the path, the coefficients a, b, and c can be determined.

In order to generalize this procedure slightly, we write instead

$$P_{pb} = aW_{tot}^2 + bW_{tot} + c. \tag{17}$$

This allows for cases in which the density or even some of the other parameters in the calculation are varying in time, during the current ramp phase of CIT for example. If most of the heating is done during the flattop, we can still use a POPCON to obtain an estimate of P_m.

We now assume we know $P_{pb}(W_0) = P_0$ and $P_{pb}(W_1 > W_0) = P_1$ and the maximum value of P_{pb} between W_0 and W_1, P_m. We allow P_0 and P_1 to be nonzero to account for cases in which ohmic ignition is possible. If the system has energy W_i at time t_i, and a constant auxiliary power P_{aux} is applied until the energy reaches W_f at time t_f, we can integrate Eq. (2)

using Eqs. (15) and (17) to obtain

$$t_f - t_i = \frac{W_1 - W_0}{\sqrt{\Delta P_a}\left(\sqrt{\Delta P_0} + \sqrt{\Delta P_1}\right)} \times \left[\tan^{-1}\left\{\left(\sqrt{\frac{\Delta P_0}{\Delta P_a}} + \sqrt{\frac{\Delta P_1}{\Delta P_a}}\right)\left[\frac{W - \overline{W}}{W_1 - W_0}\right] + \frac{1}{2}\left(\sqrt{\frac{\Delta P_1}{\Delta P_a}} - \sqrt{\frac{\Delta P_0}{\Delta P_a}}\right)\right\}\right]_{W_i}^{W_f}, \tag{18}$$

where

$$\begin{aligned} \overline{W} &\equiv (W_0 + W_1)/2, \\ \Delta P_0 &\equiv P_m - P_0, \\ \Delta P_1 &\equiv P_m - P_1, \\ \Delta P_a &\equiv P_{aux} - P_m. \end{aligned}$$

In the limit of $P_{aux} \gg P_m$, Eq. (18) becomes

$$t_f - t_i \simeq \frac{W_f - W_i}{P_{aux}}, \tag{19}$$

as expected.

If we take Eq. (17) to hold for all W_{tot}, as if P_α would continue to dominate P_{con} with increasing T, $W_{tot} \to \infty$ in a finite time. This defines a characteristic time to heat to ignition,

$$t_f - t_i \sim \frac{\pi}{2} \frac{W_1 - W_0}{\sqrt{\Delta P_a}\left(\sqrt{\Delta P_0} + \sqrt{\Delta P_1}\right)}. \tag{20}$$

In this expression, ΔP_a represents the excess input power; ΔP_0 and ΔP_1 describe the steepness of $P_{pb}(W_{tot})$ and are thus directly related to the rate at which the thermal instability proceeds.

Typical numbers for an ignited CIT would be (as in Fig. 3) $W_f - W_i \sim W_1 - W_0 \sim 50$ MJ, $P_1 \simeq P_0 \simeq 0$, and $P_m \simeq 10$ MW. For convenience we have set $W_i = W_0$ and $W_f = W_1$. With these values and $P_{aux} = 20$ MW, Eq. (18) and Eq. (20) yield exactly the same result, $t_f - t_i = 4$ s.

For most ignited CIT cases, $P_m < 10$ MW (see Sec. IV.B), and we may even have $P_m \lesssim 0$ (ohmic ignition). In this case, Eq. (19) provides an approximate lower limit to the time required to heat the plasma: $t_f - t_i \simeq 2.5$ s.

Returning now to Table I, using $t_i \simeq 5$ s, and setting t_f in the ignited cases equal to the heating off time, we see that the range $t_f - t_i = 2.5$ - 4 s also describes our numerical calculations fairly well.

We now consider cases with finite Q. In this instance, the path from ohmic equilibrium to the final state is one of monotonically increasing P_{pb}, as in the moderate-density, high-temperature region of Fig. 3. For small c_τ, the conducted losses dominate for all temperatures above ohmic equilibrium provided $\langle n_e \rangle$ is not so large as to make radiation dominant. In the limit of $c_\tau \to 0$, $P_{pb} \propto \langle T \rangle^2$ (assuming $\tau_E \propto P_{in}^{-0.5}$). The finite Q cases examined in Table I have more moderate c_τ. For them, the alpha power effectively reduces the rate of rise of P_{pb} below $\langle T \rangle^2$.

We model these cases qualitatively by linearly interpolating between two points on the POPCON. We specify the plasma energy at ohmic equilibrium, W_{OH}, and the energy attained in the limit $t \to \infty$ for a given P_{aux}, $W_{P_{aux}}$. Thus,

$$P_{pb}(W_{tot}) = \left(\frac{W_{tot} - W_{OH}}{W_{P_{aux}} - W_{OH}} \right) P_{aux}. \tag{21}$$

Integration of Eq. (2) using Eqs. (15) and (21) with initial and final energies W_i and W_f, respectively, yields

$$t_f - t_i = \frac{W_{P_{aux}} - W_{OH}}{P_{aux}} \ln \left(\frac{1 - W_i/W_{P_{aux}}}{1 - W_f/W_{P_{aux}}} \right). \tag{22}$$

Note that the time required to heat the plasma diverges logarithmically as W_f approaches $W_{P_{aux}}$.

To provide some typical values for these quantities, we give in Table II data from the $Q \sim 7$ - 10 runs of Sec. III. We evaluate t_i and W_{OH} at the earliest time for which $P_{aux} > P_{OH}$. Since Q increases roughly like W_{tot}^2, we assume $W_f = 0.95 W_{P_{aux}}$ in Table II so that we can compare with the $t(0.9Q_{max})$ entry in Table I. This is meant only as a qualitative comparison since the above model is considerably simpler than the one used in the actual numerical calculations.

In Table II, we see that, the "time required to heat the plasma" is roughly 2.5 to 3.5 s, as was the case for the ignited discharges. We reiterate that this is the result of judicious choices of $\langle n_e \rangle$ and P_{aux} and does not necessarily indicate any fundamental limitation. The effects of these choices are evident in each of Eqs. (18) - (20), and (22). The thermal inertia of the plasma increases linearly with $\langle n_e \rangle$, and the heating time decreases uniformly with P_{aux}. Between these two parameters, there is enough freedom to arrange for $t_f - t_i$ to fall within the range desired for CIT.

IV.B. Saddle Point Conditions

POPCON diagrams computed for CIT with the Kaye-Allen-Complex scaling typically yield $P_m < 10$ MW when the minimum density for ignition is below the density limit. We now use P_m to refer specifically to the power required to maintain steady state at the saddle point[6,9,18] of the POPCON. This is the absolute minimum power required for ignition. By applying the results of Waltz, Dominguez, and Perkins[5] to the present situation, we can demonstrate that this relatively small value of P_m is a general result.

In the calculation described in Ref. 5, P_{OH} is neglected, a simplified expression for P_α is used (we insert the formula proposed in Ref. 9), and the energy confinement time is taken to be $\tau_E \propto \langle n_e \rangle^\zeta \langle T \rangle^{-\xi}$. The system of equations $P_m = P_{pb}$, $\partial P_{pb}/\partial \langle n_e \rangle = 0$, $\partial P_{pb}/\partial \langle T \rangle = 0$ is solved analytically for the temperature, density $\langle n_e \rangle_m$, and auxiliary power P_m at the saddle point.

For Kaye-Allen-Complex scaling, $\zeta = -0.8$ and $\xi = 1$ (see Sec. IV.C). Then,

$$\langle n_e \rangle_m = 206. \left[c_\tau^2 \left(\frac{B_T}{10\ \mathrm{T}} \right)^{0.6} \left(\frac{I_p}{11\ \mathrm{MA}} \right)^{1.7} \right]^{-5} 10^{20}\ \mathrm{m}^{-3}, \qquad (23)$$

and

$$P_m = 3.06 \times 10^4 \left[c_\tau^2 \left(\frac{B_T}{10\ \mathrm{T}} \right)^{0.6} \left(\frac{I_p}{11\ \mathrm{MA}} \right)^{1.7} \right]^{-10} \mathrm{MW}. \qquad (24)$$

The coefficients in front of each of these expressions is a complicated function of α_n and α_T; we have evaluated them at $\alpha_n = 0.58$ and $\alpha_T = 1.53$, the values used in Sections II and III. However, all of the I_p, B_T, and c_τ dependence appears explicitly in Eqs. (23) and (24).

If c_τ (or I_p and B_T) is too small, $\langle n_e \rangle_m$ is greater than the density limit value $\langle n_e \rangle_{max}$, and there is no window for ignited operation. Combining Eqs. (23) and (24) with this requirement, we obtain

$$P_m < 0.72 \left(\frac{\langle n_e \rangle_{max}}{10^{20}\ \mathrm{m}^{-3}} \right)^2. \tag{25}$$

For CIT, the density limit scaling given in Eq. (14) typically yields $\langle n_e \rangle_{max} \sim 2 - 5 \times 10^{20} \mathrm{m}^{-3}$, depending on I_p and the density profile shape. Then, $P_m \sim 3$ - 18 MW. However, this analysis has neglected P_{OH}. Near the saddle point, P_{OH} is on the order of 5 MW for CIT. As a lowest order correction, we subtract this from P_m to estimate the auxiliary power required in steady state at the saddle point: ~ -2 - 13 MW, in agreement with typical POPCON diagrams.

Another piece of information we can get out of Eqs. (23) and (24) is the approximate scaling of critical c_τ values with I_p:

$$c_\tau \propto I_p^{-0.85} B_T^{-0.3}. \tag{26}$$

As an example, assume that $c_{\tau,11}$ is required to attain some particular level of performance for the 11 MA CIT design. Then, a multiplier of $1.3 c_{\tau,11}$ is needed to obtain roughly the same performance from the 9 MA configuration. Likewise, $0.8 c_{\tau,11}$ becomes the critical value for the 13 MA machine. This trend is evident in the stagger of the c_τ values between the various machines in Table I. Note that Eq. (26) is nothing more than the requirement that τ_E remain constant when I_p and B_T are changed.

Equations (23) and (24) exhibit a high sensitivity to c_τ, and to a lesser extent, I_p and B_T. The exponents "5" and "10" in these equations correspond to $1/(1+\zeta)$ and $2/(1+\zeta)$ in the original formulas. We can see how this arises by writing $\zeta = -1 + \epsilon$. Hence (see Sec. IV.C),

$$\frac{P_{con}}{P_\alpha - P_{rad}} \propto \frac{\langle n_e \rangle^{-\epsilon}}{c_\tau^{1+\epsilon}}. \tag{27}$$

When $\epsilon \ll 1$, as is the case here, a small change in c_τ can be offset only by a large change in $\langle n_e \rangle$. Namely, to keep the ratio in Eq. (27) constant, we would require

$$\langle n_e \rangle \propto \left(c_\tau^{1+\epsilon} \right)^{\frac{-1}{1+\zeta}}, \tag{28}$$

as in Eq. (23).

Consequently, the density scaling of τ_E is critical. The exponent ζ changes greatly in a relative sense between the various L-mode scalings (see Refs. 9 and 15, for example). The values of ζ used in the Waltz, Dominguez, and Perkins drift wave-based models are completely different: $\zeta = 0$ (ion temperature gradient driven instability) and $\zeta = 1$ (dissipative trapped electron mode). Hence, we must be careful in interpreting the results of this paper. In particular, the detailed values of c_τ employed are highly dependent upon our use of the Kaye-Alt-Complex formula. Rather than viewing the 2.5 - 4 s heating time calculated in Secs. III and IV.A as pertaining to only our particular confinement scaling, we should look at it as characteristic of all scenarios having similar values of $W_f - W_i$ and P_m, regardless of the τ_E expression used.

IV.C. Energy vs. Power Form of τ_E

Theories of tokamak energy confinement generally express their results in terms of local plasma parameters, n_e and T. It is for this reason that we have been using the energy form of τ_E up to this point. On the other hand, experimental values of τ_E are most readily categorized by input power, P_{in}, and line-averaged density since they can be obtained with relatively little data analysis. In steady state, the two forms of τ_E are related by

$$P_{in} = \frac{W_{tot}}{\tau_E}. \tag{29}$$

This is equivalent to Eq. (1) when we interpret P_{in} as the net input power: $P_{in} = P_{OH} + P_\alpha + P_{aux} - P_{rad}$.

With

$$\tau_E(P_{in}) = f_\tau P_{in}^{-\gamma}, \tag{30}$$

where f_τ contains all of the nonpower dependence (including the multiplier c_τ), this procedure yields

$$\tau_E(W_{tot}) = \left(f_\tau W_{tot}^{-\gamma}\right)^{1/(1-\gamma)}. \tag{31}$$

By definition a steady-state calculation of the power balance such as a POPCON is indifferent as to which of these two forms is used. This is not the case when transient effects are of interest.

We now define $\dot{W}_{tot}$ as the value of dW_{tot}/dt obtained with $\tau_E(P_{in})$, and $\dot{W}'_{tot}$ as that found with $\tau_E(W_{tot})$. We can then show

$$\frac{\tau_E(W_{tot})}{W_{tot}}\dot{W}_{tot} = 1 + \frac{\tau_E(W_{tot})}{W_{tot}}\dot{W}'_{tot} - \left[1 + \frac{\tau_E(W_{tot})}{W_{tot}}\dot{W}'_{tot}\right]^{\gamma}. \qquad (32)$$

In the limit $\frac{\tau_E(W_{tot})}{W_{tot}}\dot{W}'_{tot} \ll 1$ (the time rate of change of the plasma energy is much less than the conducted losses), we can expand the term in brackets to obtain

$$\dot{W}_{tot} \simeq \dot{W}'_{tot}(1-\gamma). \qquad (33)$$

In the opposite limit (valid when $P_{aux} \gg P_{con}$), $\dot{W}_{tot} \simeq \dot{W}'_{tot}$.

For the cases considered in Sec. III, the first limit is more appropriate. Noting that $\gamma = 0.5$ for the Kaye-Alt-Complex scaling, we see that $\dot{W}_{tot}$ would be reduced by a factor of two if we were to use the power form of τ_E. In other words, it would take twice as long to increase W_{tot} by a specific amount.

We show in Figs. 6 and 7 calculations identical to those given in Figs. 4 and 5, respectively, but with the power form of τ_E replacing the energy form. The "heating off times" have been altered to yield the same maximum P_α. Note that the total heating times required with the power form are less than double that needed with the energy form due to finite values of $\frac{\tau_E(W_{tot})}{W_{tot}}\dot{W}'_{tot}$.

In Sec. III, we were able to arrange the parameters of the various simulations so that the desired plasma operation point could be reached within the first half of the flattop. The above result then suggests that with the power form of τ_E, we could still achieve roughly the same end states under the assumptions of Sec. III by the end of the flattop period. By examining experimental data, it may be possible to demonstrate that one of these two ways of writing τ_E is more appropriate than the other.

V. Summary

In summary, we have made an assessment of the pulse length and auxiliary heating requirements for three possible CIT designs. To this end, a time-dependent 0-D code has been developed. Our procedures have been checked by comparing against a TSC simulation of CIT. In this comparison, we have

found that the flattop power balance matches to within $\sim$ 10 MW out of $\sim$ 100 MW for each of the dominant terms.

The primary results of this paper are contained in Table I where we have presented parameters from several simulations of each of the suggested CIT magnetic configurations. The most critical quantity in determining CIT performance is the L-mode multiplier, c_τ, defined in Eq. (13).

We can attempt to summarize Table I as follows. For the smallest values of c_τ examined in each machine, $P_{aux} = 40$ MW is required to achieve $P_\alpha \sim 60$ MW. While $P_{aux} = 20$ MW is sufficient to reach similar values of Q, $Q \gtrsim 7$, the resulting P_α is, of course, proportionately smaller. For the larger values of c_τ, $Q \gg 1$ or ignited operation is obtained with $P_{aux} \leq 20$ MW. The freedom to adjust P_{aux} and the plasma density has allowed us to reach these final plasma operating states during the first half of the current flattop.

Several analytic calculations have been presented. We first described simple models for the time required to heat the plasma, one for ignited cases and one for finite Q operation. In both instances, application of the formulas to typical CIT scenarios yielded heating times of 2.5 - 4 s, in qualitative agreement with Table I.

We then examined the minimum power required to reach ignition using expressions derived by Waltz, Dominguez, and Perkins.[5] For the Kaye-Alt-Complex τ_E scaling, we were able to show that this auxiliary heating power is $P_{aux} \lesssim 10$ MW. The equations used to do this demonstrate a high sensitivity to the value of c_τ.

This sensitivity is directly related to the density scaling exponent of τ_E. Since this quantity is somewhat uncertain,[15] we conclude that the detailed results of Table I should be used with caution. Our numerical results are, however, applicable in a qualitative sense to other situations providing a similar level of energy confinement.

Finally, we have considered the consequences of writing τ_E in terms of the input power rather than the plasma energy, as was done throughout the rest of the paper. We have found that with the former, the time required to heat the plasma through a given range of plasma energy is almost twice as long as for the latter. Since the simulations of Sec. III required less than about 4 s to heat to the desired operating point, we would still be able to reach roughly the same final states by the end of the flattop even if this more

pessimistic scaling is the appropriate description of the plasma.

Acknowledgments

The authors would like to acknowledge the numerous comments on this work provided by the CIT team. This work was supported by U.S. DOE Contract No. DE-AC02-76-CHO-3073.

References

[1]G. BATEMAN et al., "CIT Physics and Engineering Basis," *Proc. 12th Int. Conf. Plasma Physics and Controlled Nuclear Fusion*, Nice, France, November 1988, paper IAEA-CN-50/G-2-1, International Atomic Energy Agency; see also J. A. SCHMIDT and H. P. FURTH, "Compact Ignition Tokamak Conceptual Design Report," A-860606-P-01, Princeton Plasma Physics Laboratory (June 1986).

[2]D. P. STOTLER and G. BATEMAN, "Time-Dependent Simulations of a Compact Ignition Tokamak," *Fusion Technol.* **15**, 12 (1989).

[3]C. E. SINGER, L.-P. KU, and G. BATEMAN, "Plasma Transport in a Compact Ignition Tokamak," *Fusion Technol.* **13**, 543 (1988).

[4]D. P. STOTLER, R. J. GOLDSTON, and the CIT Team, "Ignition Probabilities for CIT," Princeton Plasma Physics Laboratory Report No. PPPL-2629 (1989); *Fusion Technol.* (to be published).

[5]R. E. WALTZ, R. R. DOMINGUEZ, and F. W. PERKINS, "Drift Wave Model Tokamak Ignition Projections with a Zero-Dimensional Transport Code," *Nucl. Fusion* **29**, 351 (1989).

[6]N. A. UCKAN and J. SHEFFIELD, "A Simple Procedure for Establishing Ignition Conditions in Tokamaks," *Tokamak Startup*, p. 45, H. KNOEPFEL, Ed., Plenum Press, New York (1986).

[7]Y. C. SUN, D. E. POST, G. BATEMAN, and D. STOTLER, "The Performance of CIT and ITER Under Various Scaling Laws," *Bull. Am. Phys. Soc.* **33**, 1971 (1988).

[8]O. MITARAI, A. HIROSE, and H. M. SKARSGARD, "Generalized Ignition Contour Map and Scaling Law Requirement for Reaching Ignition in a Tokamak Reactor," *Nucl. Fusion* **28**, 2141 (1988).

[9]N. A. UCKAN, "Relative Merits of Size, Field, and Current on Ignited Tokamak Performance," *Fusion Technol.* **14**, 299 (1988).

[10]L. M. HIVELY, "Convenient Computational Forms for Maxwellian Reactivities," *Nucl. Fusion* **17**, 873 (1977).

[11]S. C. JARDIN, N. POMPHREY, and J. DE LUCIA, *J. Comput. Phys* **66**, 481 (1986).

[12]N. POMPHREY, "The 11 MA Fiducial Discharge," Compact Ignition Tokamak Report AE-890417-PPL-04 (1989).

[13]S. C. JARDIN, J. DE LUCIA, M. OKABAYASHI, N. POMPHREY, M. REUSCH, S. KAYE, and H. TAKAHASHI, "Post-Disruptive Plasma Loss in the Princeton Beta Experiment (PBX)," *Nucl. Fusion* **27**, 569 (1987).

[14]W. M. TANG, "*Microinstability-Based Model for Anomalous Thermal* Confinement in Tokamaks," *Nucl. Fusion* **26**, 1605 (1986).

[15]S. M. KAYE, "Survey of Energy Confinement Scaling Expressions," presented at the *ITER Specialists' Meeting on Energy Confinement*, 24-27 May 1988, Garching, Federal Republic of Germany.

[16]S. M. KAYE, Princeton Plasma Physics Laboratory, Private Communication (1989).

[17]JET Team, "JET Latest Results and Future Prospects," *Proc. 12th Int. Conf. Plasma Physics and Controlled Nuclear Fusion*, Nice, France, November 1988, paper IAEA-CN-50/A-1-3, International Atomic Energy Agency.

[18]W. A. HOULBERG, S. E. ATTENBERGER, and L. M. HIVELY, "Contour Analysis of Fusion Reactor Plasma Performance," *Nucl. Fusion* **22**, 935 (1982).

	P_{aux}	$\langle n_{e,20} \rangle$	$P_{\alpha,max}$	Q_{max}	heating off time	$t(P_{\alpha,max})$ or $t(0.9Q_{max})$
$I_p = 9$ MA						
$c_\tau = 1.6$	20	2.2	31	7.7	-	8.7
	40	3.2	69	8.6	-	8.3
$c_\tau = 1.9$	10	2.6	44	22.	-	11.3
	20	3.5	82	41. (@ 10 MW)	-	9.6
$c_\tau = 2.2$	10	3.5	56	∞	9.6	12.0
	20	3.5	171	∞	7.5	11.7
$I_p = 11$ MA						
$c_\tau = 1.3$	20	2.2	36	8.9	-	8.5
	40	3.3	80	10.	-	8.3
$c_\tau = 1.6$	20	3.8	106	266. (@ 2 MW)	-	8.7
	30	4.3	120	∞	7.8	8.5
$c_\tau = 1.9$	10	4.3	135	∞	8.7	12.0
	20	4.3	333	∞	7.5	9.3
$I_p = 13$ MA						
$c_\tau = 1.0$	20	2.1	27	6.7	-	8.3
	40	3.0	56	7.0	-	8.1
$c_\tau = 1.3$	10	3.0	54	68. (@ 4 MW)	-	10.9
	30	4.6	151	∞	8.2	8.3
$c_\tau = 1.6$	10	5.1	241	∞	8.9	12.0
	20	5.1	492	∞	7.5	9.3

Table I: Parameters for each of the 18 time-dependent simulations.

I_p	c_τ	P_{aux}	W_{OH}	$W_{P_{aux}}$	$t(0.95W_{P_{aux}})$
9	1.6	20	5.5	30	8.3
9	1.6	40	6.2	46	7.5
11	1.3	20	6.4	33	8.5
11	1.3	40	9.2	48	7.6
13	1.0	20	8.6	28	7.7
13	1.0	40	9.4	41	7.1

Table II: Time required to heat plasma to 95% of $W_{P_{aux}}$ evaluated using data from Table I and Eq. (22).

Figures

FIG. 1. Time dependence of various CIT parameters taken from TSC simulation Fi1D1; units are given separately for each.

FIG. 2. Time dependence of the various terms in Eq. (2). The solid lines are the result of the 0-D calculation. The markers indicate corresponding values taken from TSC output. Note that several of these points have been deleted for clarity. The solid squares represent P_{OH} from TSC; the diamonds are for P_{aux}.

FIG. 3. Contours of constant auxiliary power in MW in $\langle n_e \rangle$ and $\langle T \rangle$ space for the 11 MA design with $c_\tau = 1.6$. The density and β limits are indicated.

FIG. 4. Time dependence of the various terms in Eq. (2) for the 11 MA configuration of CIT with $c_\tau = 1.6$ and $\langle n_e \rangle = 3.8 \times 10^{20}$ m^{-3}.

FIG. 5. Time dependence of the various terms in Eq. (2) for the 11 MA configuration of CIT with $c_\tau = 1.6$ and $\langle n_e \rangle = 4.3 \times 10^{20}$ m^{-3}.

FIG. 6. Time dependence of the various terms in Eq. (2) for the 11 MA configuration of CIT with $c_\tau = 1.6$ (using the power- dependent form of τ_E) and $\langle n_e \rangle = 3.8 \times 10^{20}$ m^{-3}.

FIG. 7. Time dependence of the various terms in Eq. (2) for the 11 MA configuration of CIT with $c_\tau = 1.6$ (using the power- dependent form of τ_E)and $\langle n_e \rangle = 4.3 \times 10^{20}$ m^{-3}.

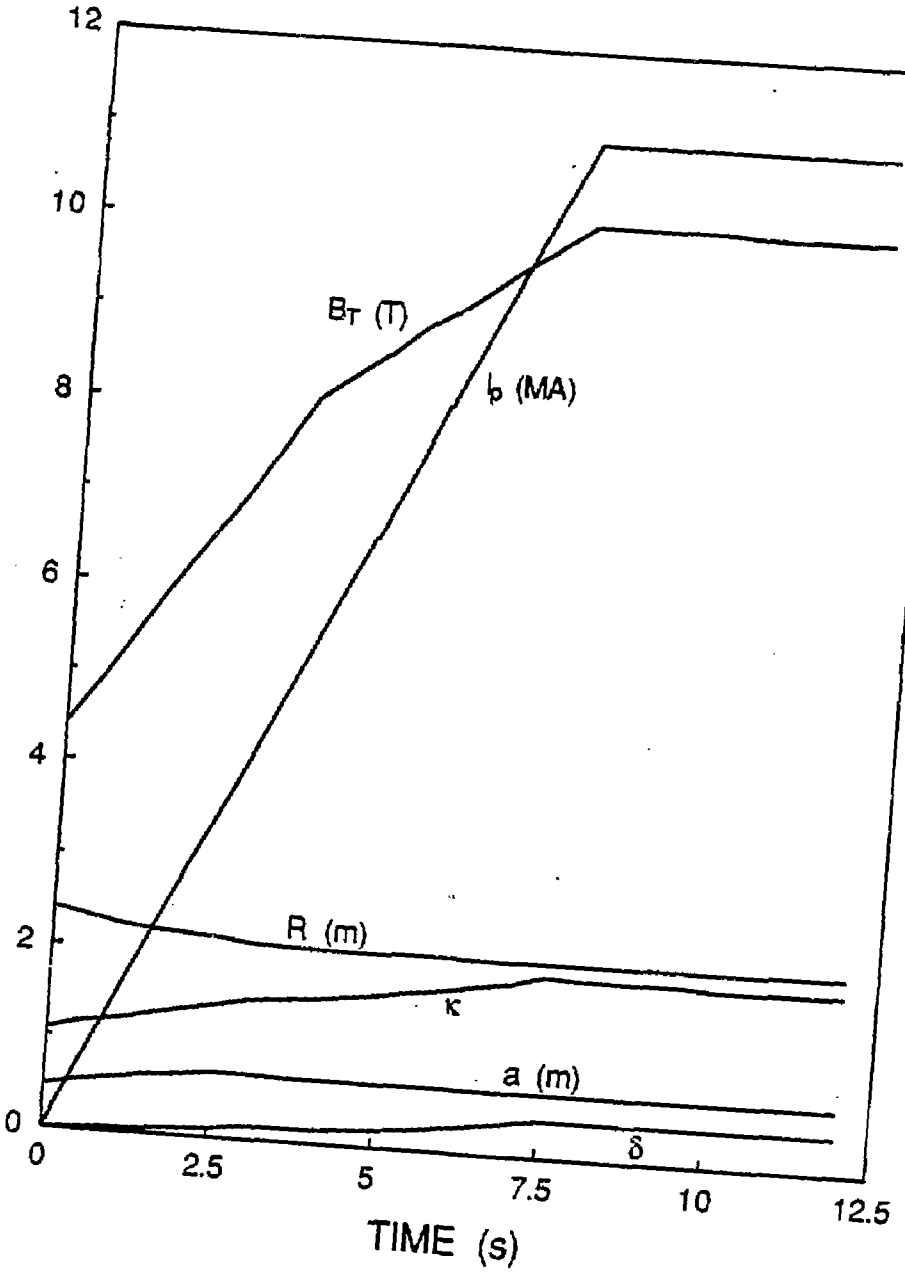

FIG. 1

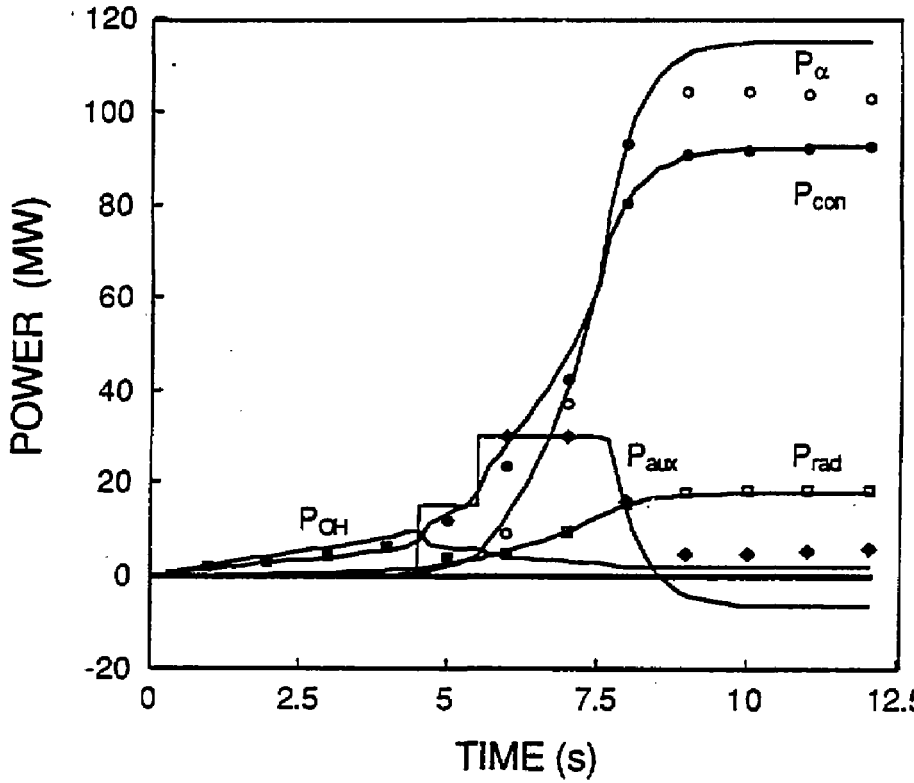
120
100
80
60
40
20
0
-20
POWER (MW)
0
2.5
5
7.5
10
12.5
TIME (s)
P_α
P_{con}
P_{aux}
P_{rad}
P_{OH}

FIG. 2

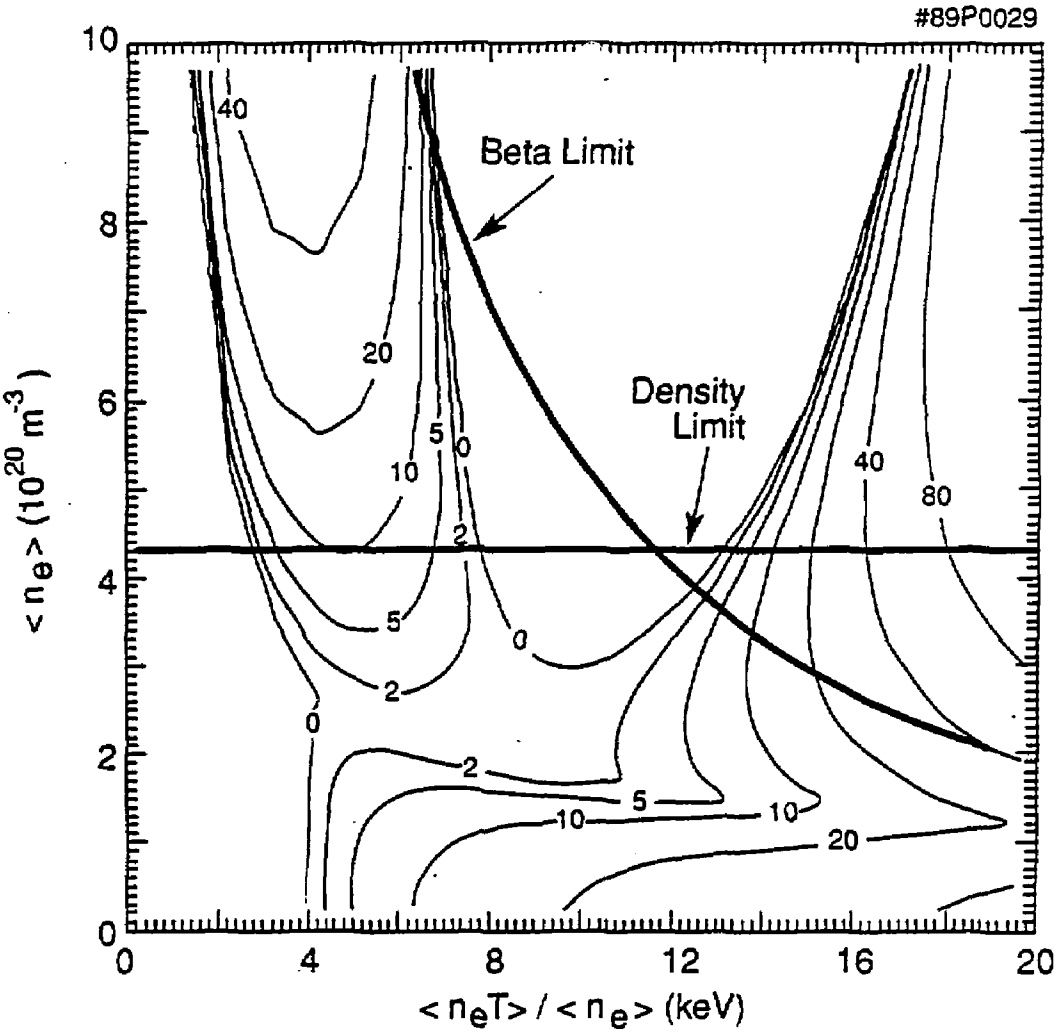
#89P0029
Beta Limit
Density Limit
40
20
10
5
2
0
80
$< n_e > (10^{20} m^{-3})$
$< n_e T > / < n_e >$ (keV)
0
2
4
6
8
10
12
16
20

FIG. 3

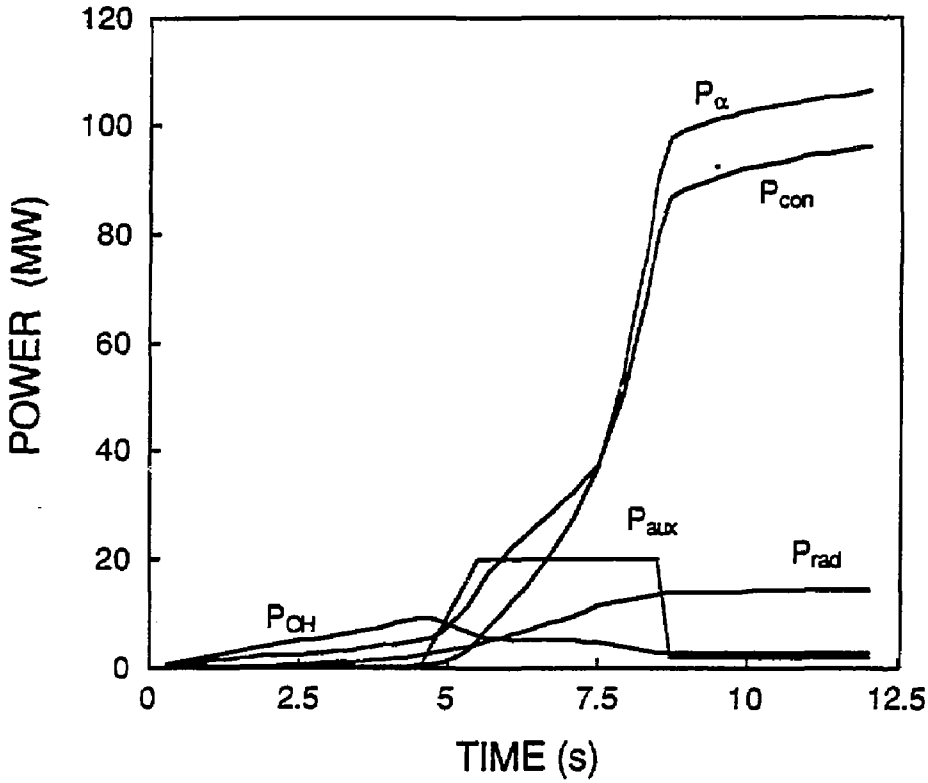
120
100
80
60
40
20
0
POWER (MW)
0
2.5
5
7.5
10
12.5
TIME (s)
P_α
P_{con}
P_{aux}
P_{rad}
P_{OH}

FIG. 4

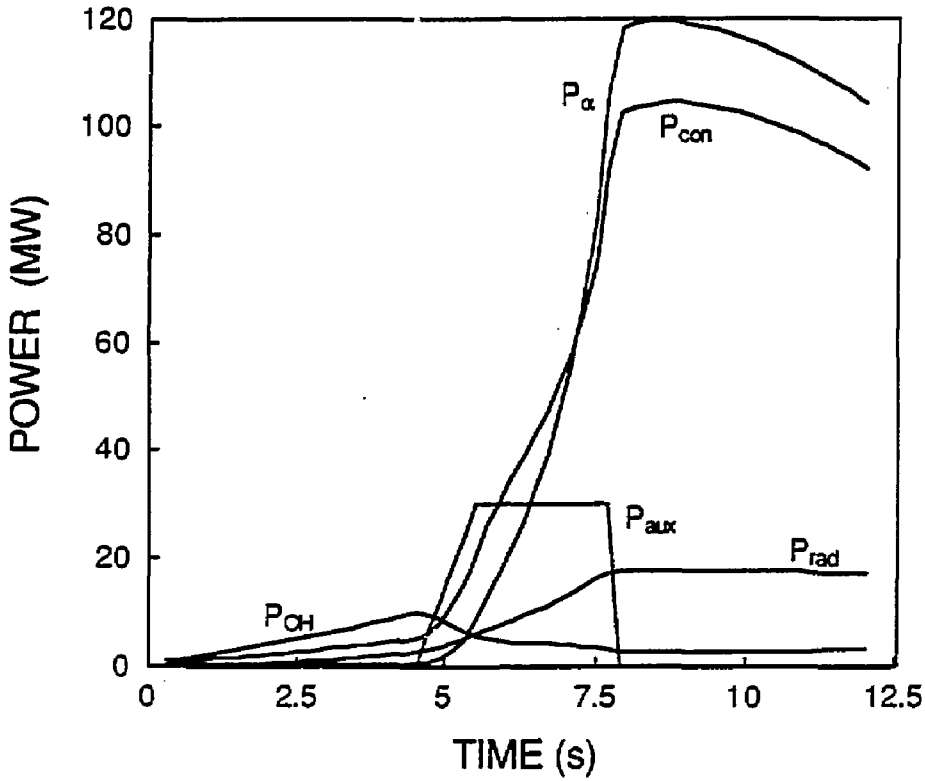
120
100
80
60
40
20
0
POWER (MW)
0
2.5
5
7.5
10
12.5
TIME (s)
P_α
P_{con}
P_{aux}
P_{rad}
P_{OH}

FIG. 5

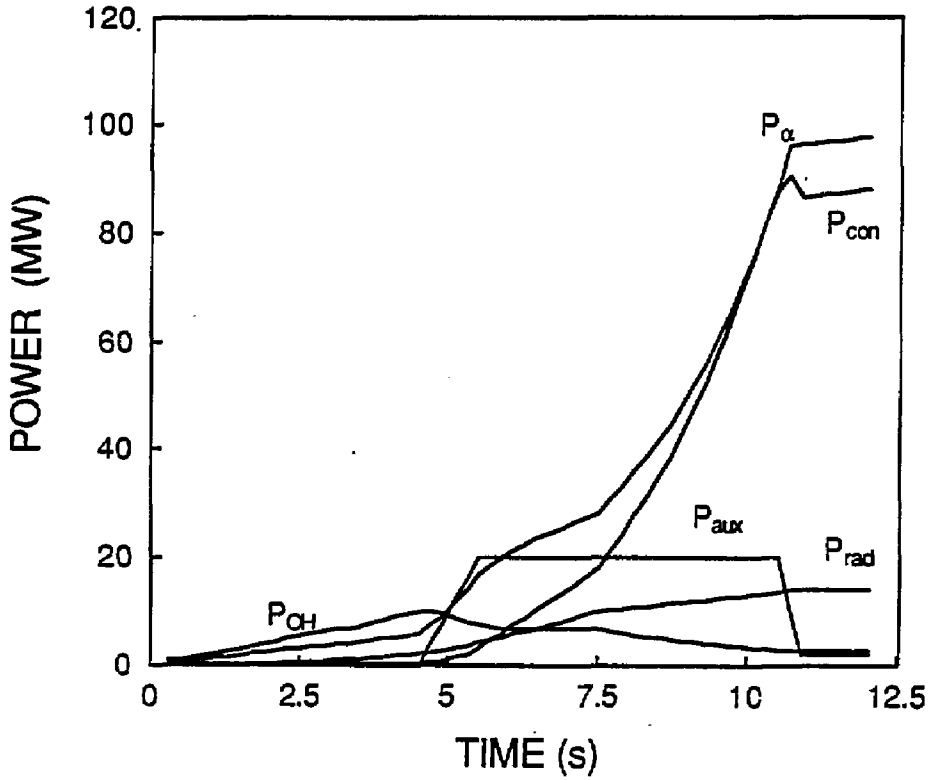
120
100
80
60
40
20
0
POWER (MW)
0
2.5
5
7.5
10
12.5
TIME (s)
P_α
P_{con}
P_{aux}
P_{rad}
P_{OH}

FIG. 6

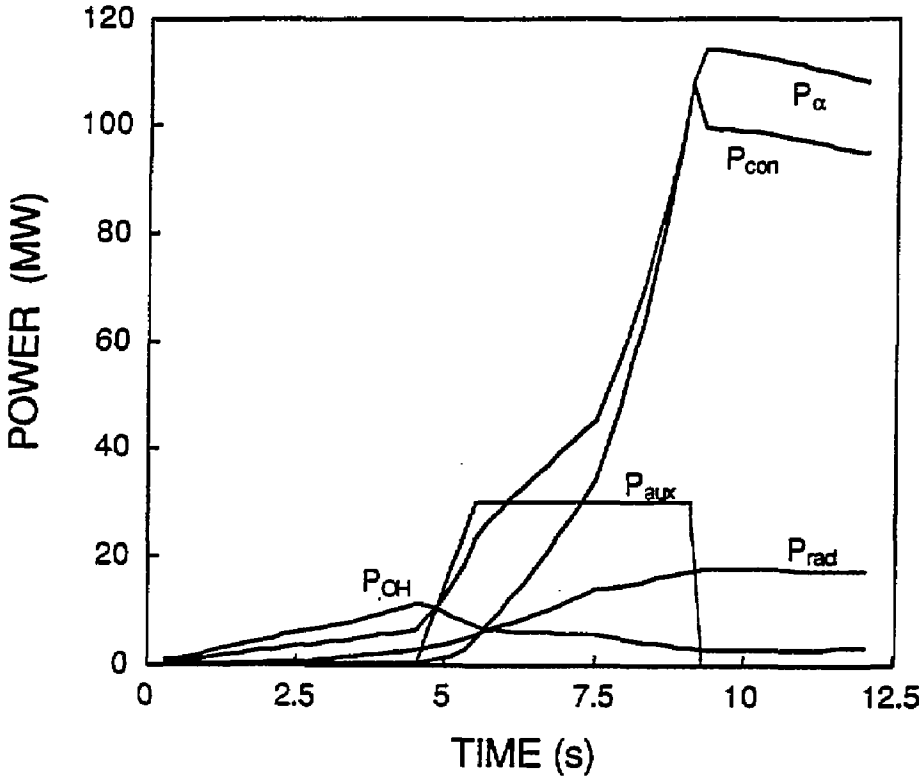
120
100
80
60
40
20
0
POWER (MW)
0
2.5
5
7.5
10
12.5
TIME (s)
P_α
P_{con}
P_{aux}
P_{rad}
P_{OH}

FIG. 7

EXTERNAL DISTRIBUTION IN ADDITION TO UC-420

Dr. Frank J. Paoloni, Univ of Wollongong, AUSTRALIA
Prof. M.H. Brennan, Univ Sydney, AUSTRALIA
Plasma Research Lab., Australian Nat. Univ., AUSTRALIA
Prof. I.R. Jones, Flinders Univ., AUSTRALIA
Prof. F. Cap, Inst Theo Phys, AUSTRIA
Prof. M. Heindler, Instut fur Theoretische Physik, AUSTRIA
M. Goossens, Astronomisch Instituut, BELGIUM
Ecole Royale Militaire, Lab de Phys Plasmas, BELGIUM
Commission-European, Dg-XII Fusion Prog, BELGIUM
Prof. R. Boucique, Rijksuniversiteit Gent, BELGIUM
Dr. P.H. Sakanaka, Instituto Fisica, BRAZIL
Instituto De Pesquisas Espaciasi-INPE, BRAZIL
Documents Office, Atomic Energy of Canada Limited, CANADA
Dr. M.P. Bachynski, MPB Technologies, Inc., CANADA
Dr. H.M. Skarsgard, University of Saskatchewan, CANADA
Dr. H. Barnard, University of British Columbia, CANADA
Prof. J. Teichmann, Univ. of Montreal, CANADA
Prof. S.R. Sreenivasan, University of Calgary, CANADA
Prof. Tudor W. Johnston, INRS-Energie, CANADA
Dr. Bolton, Centre canadien de fusion magnetique, CANADA
Dr. C.R. James, Univ. of Alberta, CANADA
Dr. Peter Lukac, Komenskeho Univ, CZECHOSLOVAKIA
The Librarian, Culham Laboratory, ENGLAND
The Librarian, Rutherford Appleton Laboratory, ENGLAND
Mrs. S.A. Hutchinson, JET Library, ENGLAND
C. Mouttet, Lab. de Physique des Milieux Ionises, FRANCE
J. Radet, CEN/CADARACHE - Bat 506, FRANCE
Ms. C. Rinni, Librarian, Univ. of Ioannina, GREECE
Dr. Tom Mual, Academy Bibliographic Ser., HONG KONG
Preprint Library, Hungarian Academy of Sciences, HUNGARY
Dr. B. Das Gupta, Saha Inst of Nucl. Phys., INDIA
Dr. P. Kaw, Institute for Plasma Research, INDIA
Dr. Philip Rosenau, Israel Inst. of Tech, ISRAEL
Librarian, Int'l Ctr Theo Phys, ITALY
Prof. G. Rostagni, Istituto Gas Ionizzati Del CNR, ITALY
Miss Clelia De Palo, Assoc EURATOM-ENEA, ITALY
Dr. G. Grosso, Istituto di Fisica del Plasma, ITALY
Dr. H. Yamato, Toshiba Res & Dev, JAPAN
Prof. T. Kawakami, Atomic Energy Res. Institute, JAPAN
Prof. Kyoji Nishikawa, Univ of Hiroshima, JAPAN
Director, Dept. Large Tokamak Res. JAERI, JAPAN
Prof. Satoshi Itoh, Kyushu University, JAPAN
Research Info Center, Nagoya University, JAPAN
Prof. S. Tanaka, Kyoto University, JAPAN
Library, Kyoto University, JAPAN
Prof. Nobuyuki Inoue, University of Tokyo, JAPAN
S. Mori, JAERI, JAPAN
H. Jeong, Librarian, Korea Advanced Energy Res Inst, KOREA
Prof. D.I. Choi, The Korea Adv. Inst of Sci & Tech, KOREA
Prof. B.S. Liley, University of Waikato, NEW ZEALAND
Institute of Plasma Physics, PEOPLE'S REPUBLIC OF CHINA
Librarian, Institute of Phys., PEOPLE'S REPUBLIC OF CHINA
Library, Tsing Hua University, PEOPLE'S REPUBLIC OF CHINA
Z. Li, Southwest Inst. Physics, PEOPLE'S REPUBLIC OF CHINA
Prof. J.A.C. Cabral, Inst Superior Tecnico, PORTUGAL
Dr. Octavian Petrus, AL I CUZA University, ROMANIA
Dr. Jan de Villiers, Fusion Studies, AEC, SO AFRICA
Prof. M.A. Hellberg, University of Natal, SO AFRICA
C.I.E.M.A.T., Fusion Div. Library, SPAIN
Dr. Lennart Stenflo, University of UMEA, SWEDEN
Library, Royal Institute of Tech, SWEDEN
Prof. Hans Wilhelmson, Chalmers Univ of Tech, SWEDEN
Centre Phys des Plasmas, Ecole Polytech Fed, SWITZERLAND
Bibliotheek, Fom-Inst Voor Plasma-Fysica, THE NETHERLANDS
Metin Durgut, Middle East Technical University, TURKEY
Dr. D.D. Ryutov, Siberian Acad Sci, USSR
Dr. G.A. Eliseev, Kurchatov Institute, USSR
Dr. V.A. Glukhikh, Inst Electrophysical Apparatus, USSR
Prof. O.S. Padichenko, Inst. of Phys. & Tech. USSR
Dr. L.M. Kovrizhnykh, Institute of Gen. Physics, USSR
Nuclear Res. Establishment, Julich Ltd., W. GERMANY
Bibliothek, Inst. Fur Plasmaforschung, W. GERMANY
Dr. K. Schindler, Ruhr-Universitat Bochum, W. GERMANY
ASDEX Reading Rm, c/o Wagner, IPP/Max-Planck, W. GERMANY
Librarian, Max-Planck Institut, W. GERMANY
Prof. R.K. Janev, Inst of Phys, YUGOSLAVIA